APPLIED GEOPHYSICS, Vol.6, No.4 (December 2009), P. 359 - 366, 8 Figures.
DOI:10.1007/s11770-009-0043-9

Ordovician limestone aquosity prediction using nonlinear seismic attributes: Case from the Xutuan coal mine

Huang Yaping[1], Dong Shouhua[2], and Geng Jianhua[1]

Abstract: Ordovician limestone water is the main source of water inrush in North China coal mines. In this paper, we analyze the characteristic of three kinds of nonlinear seismic attributes, such as the largest lyapunov exponent,fractal dimension and entropy and introduce their calculation methods. Taking the 81st and 82nd coal districts in the Xutuan coal mine as examples, we extract the three seismic attributes based on the 3D prestack migration seismic data of this area, which can display the Ordovician limestone fracture distribution in the mine. We comprehensively analyzed the three nonlinear seismic attributes and compared the results with transient electromagnetic exploration results and determined the possible Ordovician limestone aquosity distribution. This demonstrated that the nonlinear seismic attributes technology is an effective approach to predict the aquosity of Ordovician limestone.
Keywords: nonlinear seismic attribute, limestone, aquosity, prediction

Introduction

In China, coal fields have a wide geographical distribution and exhibit complex hydro-geological conditions and diverse types. In coal mine accidents, water damage is second only to gas accidents (Ge and Ye, 2001). Most of the coal mines in northern China are subject to threat from coal seam water. For example, during coal mining, the inrush of water often occurs in the coal seam roof and floor, which greatly affects the security of the coal production. The water inrush mainly is from Ordovician limestone water (Wang and Wen, 1996; Yang et al., 2002). Therefore, researching the aquosity of coal mine Ordovician limestone has great significance for preventing water inrush of coal seam roof and floor. The Ordovician limestone water mainly is in the cracks and fractured zones. Methods for predicting Ordovician limestone aquifer mainly use inversion and seismic attribute technology. Many scholars at home and abroad carried out active research on the Ordovician limestone fractures. Lawrence (1998) used angle and coherence properties of the reservoir to successfully predict small faults. Chopra and Marfurt (2005; 2006b; 2007) and Liu and Marfurt (2007) have applied seismic attributes to the detection of faults and cracks and reservoir prediction, achieving good results. Sukmono (2007) successfully applied seismic multiple attributes to lithology and porosity prediction. Dong et al. (2004) and Dong (2008) successfully predicted seam cracks based on pre-stack seismic attributes and have done research on coalfield horizontal seismic prediction. Li and Meng (2004) have researched karst fracture zones using seismic attribute technology.

Theoretical studies have shown that geological bodies containing fluids such as water will cause seismic wave scatter and energy attenuation. The velocity and density of water in the Ordovician limestone aquifer are

Manuscript received by the Editor January 11, 2009; revised manuscript received November 17, 2009.
1. School of Ocean and Earth Science, TongJi University, Shanghai 200092, China.
2. School of Resource and Earth Science, China University of Mining and Technology, Xuzhou 221008, China.

lower than in the surrounding rock (Wang et al., 2000; Lue, 2001; Liu et al. 2002; Guo, 2005). The spatial changes of nonlinear seismic attributes also reflect changes of geological bodies, so we can use nonlinear seismic attributes to analyze the aquosity of Ordovician limestone. Thus, we can predict the Ordovician limestone aquifer in order to prevent the inrush of water from the coal seam roof and floor during coal mining,

Nonlinear seismic attribute analysis

Previously, conventional seismic attributes, such as amplitude, frequency, and other attributes were used to predict the aquosity of Ordovician limestone, which yielded some results. In this paper, we predict the fracture zones using three nonlinear seismic attributes and then predict the aquosity of the Ordovician limestone.

The largest Lyapunov exponent attribute

Chaos is a common phenomenon existing in nonlinear dissipative systems. It seems to have random characteristics. At present, the methods for describing the chaos phenomenon include frequency division sampling, power spectral analysis, Poincare section, and the largest Lyapunov exponent. The largest Lyapunov exponent is widely used to describe the speed characteristics (fast or slow) of exponent separation in phase-space orbit. On the one hand, it can portray whether the sequence is chaotic or not and, on the other hand, if the system is chaotic, it also can portray the complexity of the system. Sedimentary basins are dissipative nonlinear dynamic systems and when contain water, gas, and oil in reservoirs, the system can be complicated. The Lyapunov exponent on the complexity of the changes are more sensitive (Gui and Han, 2004), so using the largest Lyapunov exponent attribute can predict the fracture zone and then further predict the aquosity of Ordovician limestone.

Rosenstein et al. (1993) and Kantz (1994) proposed a convenient calculation method for small data sets (Zhang, 1996). As a result, small amounts of data can be used for calculating the largest Lyapunov exponent of short windows. The specific calculation steps are:

1. Calculate the autocorrelation of the time series. When the autocorrelation function is less than or equal to the value of experience (1-1/e), calculate the time-delay (τ) of the reconstruction phase space where e is a constant, e=2.7183.

2. Determine the optimal embedding dimension (M) of the reconstruction phase space by the false neighboring points method.

3. Reconstruct phase space $\{X_j, j = 1, 2, ..., M\}$ based on the time delay (τ) and embedding dimension (M) is the optimal embedding dimension of reconstruction phase space.

4. Find the nearest neighbor points ($X_{\bar{j}}$) of every point (X_j) in space (M). The distance of zero discrete time is

$$d_j(0) = \min_j \left\| X_j - X_{\bar{j}} \right\|. \tag{1}$$

5. For each point (x_j) of the phase space, calculate the distance after the ith neighbor point pair:

$$d_j(i) = \left\| X_{j+i} - X_{\bar{j}+i} \right\| \quad j = 1,2,...,\min(M-j, M-\bar{j}). \tag{2}$$

6. For each (i), calculate the average value ($y(i)$) $\ln d_j(i)$ of all (j):

$$y(i) = \frac{1}{p}\sum_{j=1}^{p} \ln d_j(i), \tag{3}$$

where P is the number ($x_j(k)$) of non-zero discrete time, make the regression line of $y(i)$~i using least squares and the slope of the straight line is the largest Lyapunov exponent.

Fractal dimension attribute

Rock properties and their distribution in the earth exhibit strong, non-uniform anisotropy after a long era of multiple geological effects. Within the framework of a certain scale, rocks have a disorganized, messy, scattered, and fragmented form but also show a self-similarity, i.e., fractal features. Fractal dimension is the main quantitative parameter used to describe the fractal features. It is closely related to the relative amount of corresponding geometry, physical, and chemical characteristics of the fractal body (Yi, 1995; Wu, 1995). Different lithology, fluid property, and reservoir parameters correspond to different seismic data fractal dimensions, so the fractal dimension attribute of seismic data can be used to predict the fracture zones and then predict the aquosity of the Ordovician limestone.

The correlation dimension method calculates the fractal dimension by the characteristics of the phase-space. The correlation dimension calculation needs to rearrange the time domain curve ($x_i = \{x_i\}_k$) in order to establish a vector phase space ($\{x_i\}_k$) where T is the time interval and k is dimension. If the original time series is x_1, x_2, x_3, … x_n, the phase space vector after the expansion is

$$X_1 = [x(t_1), x(t_1+T), x(t_1+2T), ..., x(t_1+(k-1)T)]$$
$$X_2 = [x(t_2), x(t_2+T), x(t_2+2T), ..., x(t_2+(k-1)T)]$$
...
$$X_I = [x(t_I), x(t_I+T), x(t_I+2T), ..., x(t_I+(k-1)T)], \quad (4)$$

where the value of M depends on the value of n, k, and τ, and I=1,2,3 … M, T is the time interval, k is the phase space dimension, and n is the number of original data,

$$D_{IJ} = \|X_I - X_J\|, \quad (5)$$

$$D_{IJ} = \sum_{l=1}^{k} |X_I(l) - X_J(l)|. \quad (6)$$

D_{IJ} is the distance of any tw o vectors X_I and X_J in the phase space above and || || represents the norm of the vector.

Arbitrarily let a positive number ($r>0$), with the proportion of point pairs with a distance of less than (r) in all point pairs is denoted by C (r). When r is very small, C (r)=0 and when r is large, C (r)=1. If the election of r is appropriate, C (r) changes with r in the form of a power function: $C(r) \propto r^d$ and we have

$$d(r) = \frac{\partial \ln C(r)}{\partial \ln r}. \quad (7)$$

Its correlation dimension is

$$D = \lim_{r \to \infty} d(r). \quad (8)$$

Entropy attribute

Entropy is a measure of disorder and chaos. The greater the entropy, the higher the degree of chaos. If a reservoir contains water, the vicinity of the water-bearing zone is generally accompanied by a fracture and the degree of disorder and chaos is higher. If entropy attribute changes appear on the section, we can predict the fracture zones and further predict the aquosity of the Ordovician limestone. Here, we adopted the method for calculating entropy proposed by Grassberger and Procaccia (1983). After establishing the phase space, we calculated the number of fractal dimension based on the algorithm of fractal dimension attribute. The entropy and fractal dimension has a relationship as

$$\log_2 C(r) = D \log_2 r - km\tau, \quad (9)$$

where we arbitrarily let a positive number ($r>0$) and the points at less than the distance (r) of all points in the proportion are recorded as C (r). D is fractal dimension, m is the dimensions of the phase space, τ is the time delay of the phase space, and k is the entropy value.

Application examples

The basic situation of the study area

The 81st and 82nd coal districts of the Xutuan coal mine belong to the subtle Permian system coalfield. Below the Cenozoic (Q+N), there are the Upper Permian Shihezi formation, Lower Permian Shihezi formation, Shanxi formation, Upper Carboniferous Taiyuan formation, Middle Carboniferous Benxi formation, and Middle and Lower Ordovician in the exploration area. The Xinhuaxia and Huaiyin arc-shaped structures are the main regional structures. The exploration area is located at the southern part of the Tongting anticline, which is an east dipping monoclonal structure with a north-southern strike. Along strike smaller folds are well developed. The primary mining coal bed is relatively flat shallow and relatively steep at depth, gradually changing with depth.

Reflection waveform characteristics

The main seismic reflection wave groups are:

T_{O+N}: the reflections from the Neocene and the basal T_{O+N} in this area can be tracked and correlated. However, due to a lot of basal conglomerates and local unconformities, some of the T_{O+N} reflections are weak and poorly continuous as shown in Figure 1.

T_7: the reflections from Coal Seam 7 below Permian. Coal seam 7 can be divided into two layers, coal seams T_{7-1} and T_{7-2}. When the coal seams merge, the reflection appears strong and continuous. On the profile in Figure 1, we can see clear bifurcation of the coal seam and obvious dynamic characteristics. The event can be continuously tracked over the whole area. It is the main target layer in this area.

T_{8-2}: the T_{8-2} reflection has strong energy and good continuity.

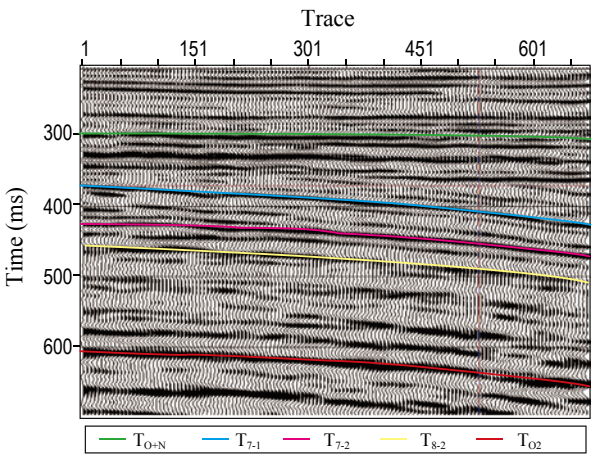

Fig. 1 The main reflections in the study area.

T_{O2}: this is the reflection from the Ordovician limestone top which has good continuity and strong energy, so it can generally be continuously tracked over the whole region.

Characteristics of the nonlinear seismic attributes

In the 81st and 82nd coal districts of the Xutuan coal mine, we collected 840 inlines (inline 80 to inline 920) of three-dimensional data and 440 crosslines (crossline 120 to crossline 560). The crossline 400 profile is shown in Figure 2 and the inline 430 profile is shown in Figures 3. In Figure 2 we see two anomalies with discontinous seismic events a and b located at inlines 280-300 and inlines 830-920. In Figure 3 we see anomalies c and d located at crosslines 220-270 and crosslines 420-470. Their seismic events are also not continuous.

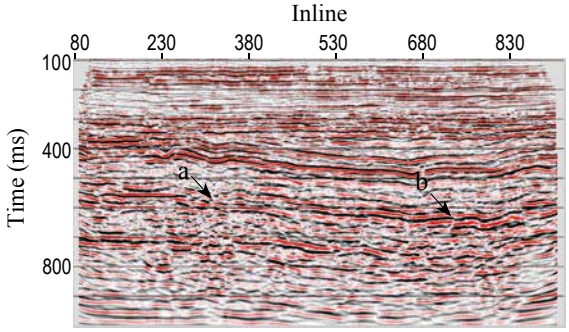

Fig. 2 Crossline 400 with anomalies a and b.

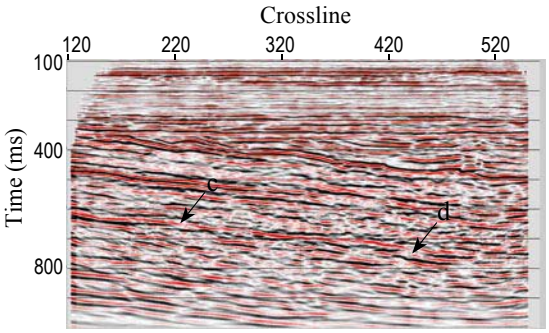

Fig.3 Inline 430 with anomalies c and d.

The anomaly a, b, and c are at approximately 600 ms time and the events appear discontinuous.

The anomaly d is at about 700 ms time and the seismic event also is not continuous. This suggests that there are fracture zones at these locations. Past experience tells us that the Ordovician limestone aquifer is generally in the fracture zones of the structure.

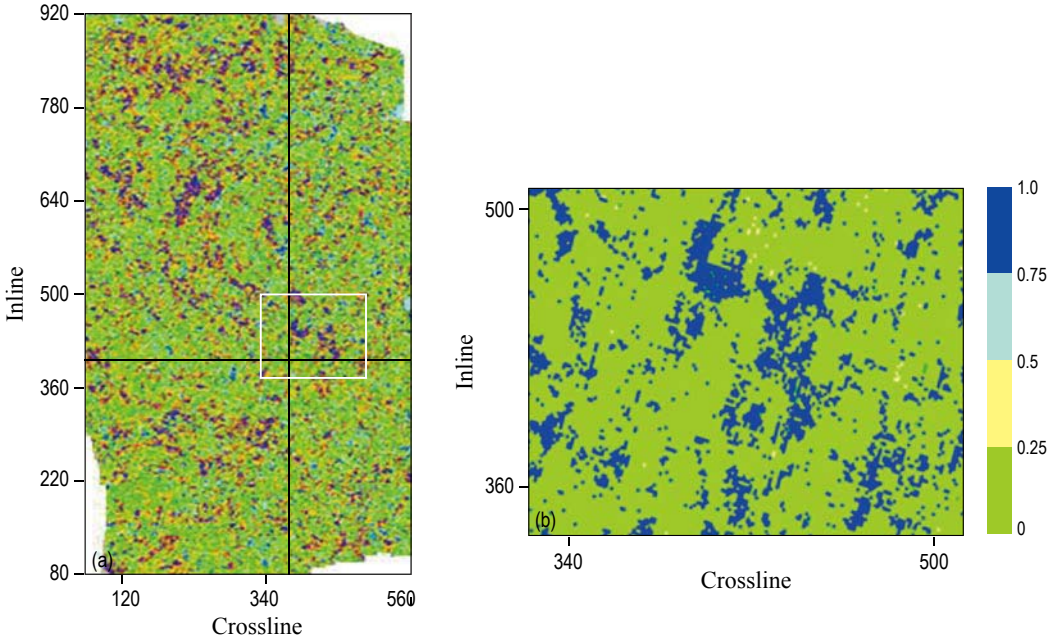

Fig.4 Plot of the largest Lyapunov Exponent attribute for the reflector T_{O2} (a) and the enlargement of the area inside the white box in Figure 4a (b). The seismic profiles of Figures 2 and 3 are indicated by black lines in Figure 4a.

Regarding the T_{O2} reflector from the 3-D data volume in the mine area as the target layer, we apply the symmetrical open window method to extract the three attributes: the largest Lyapunov exponent, fractal dimension, and entropy attributes with a window length of 30 ms. The resulting attribute plots are shown in

Figures 4 to 6. By comparative analysis of attribute changes in the three plots, we see that the attribute plot calculated from the largest Lyapunov exponent algorithm has certain regularity (Figures 4a and 4b). The size of the largest Lyapunov exponent value reflects the degree of geological complexity. The larger values indicate a more complex geological condition. The blue color in the plot shows the larger values of the largest Lyapunov exponent and is considered to be areas of fractures. The anomalies are obvious at inlines 380-430 and crosslines 370-420.

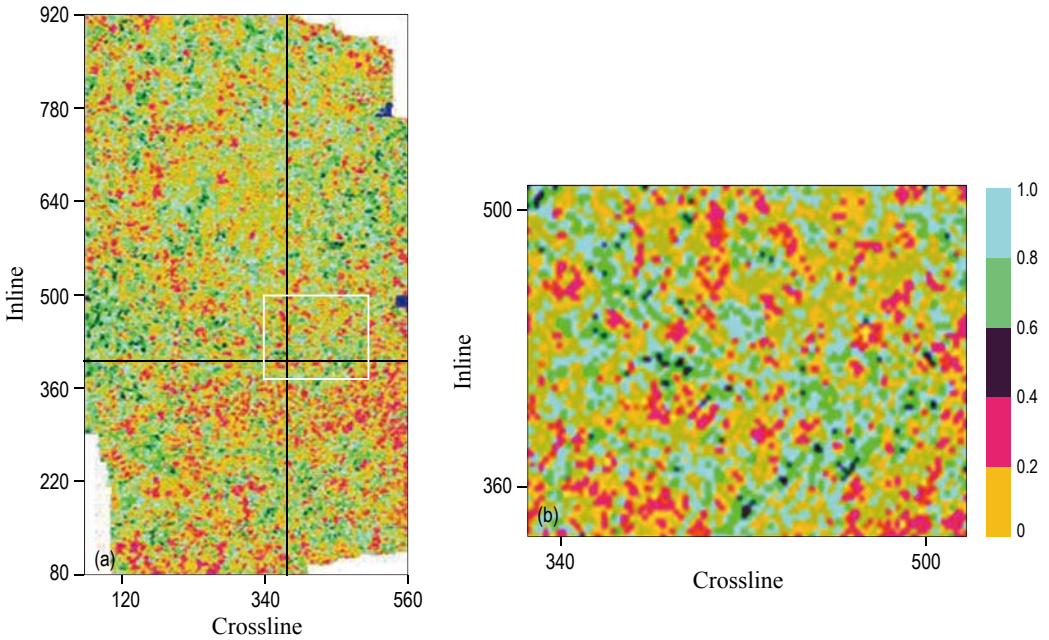

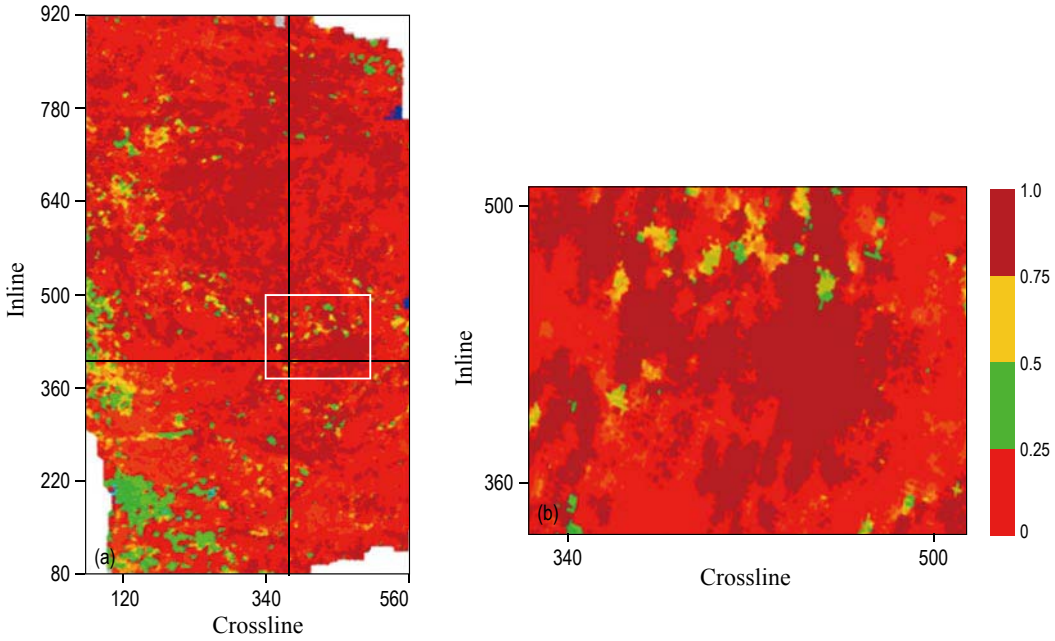

The fractal dimension attribute plot is shown in Figures 5a and 5b). The fractal dimension value is also relative to the geological complexity with the larger values indicating more complex geological conditions. The pale blue color represents larger fractal dimension values and indicates that there are fractures. However, due to seismic data limitations, the geological significance of the attribute patterns is not clear and the regularity is not obvious.

The entropy attribute plot (Figures 6a and 6b) indicates the complexity of geological conditions with larger values indicating more complex geologic conditions. The brown color indicates larger entropy values, implying that these areas are fracture zone. There is an obvious anomaly at inlines 390-420 and crosslines 380-410 and there are anomalies in the vicinity of inline 730 and crossline 370.

The anomalous areas derived from the three kinds of attribute maps are compared to the abnormal areas of Figures 2 and 3. We see that anomalies a and b in Figure 2 correspond to the predicted fracture zones shown in Figures 4 and 6. The anomalies c and d in Figure 3 correspond to the predicted fracture zones shown in Figure 5, which are more obvious at inlines 380-430 and crosslines 370-450.

Predicting limestone aquosity from the multi-attribute parameters based on electromagnetic data

We have performed transient electromagnetic exploration in the 81st and 82nd coal districts of the Xutuan coal mine. Figure 7 is the apparent resistivity distribution map observed by the transient electromagnetic exploration at 50-meter above the Ordovician limestone top. Based on the size of the apparent resistivity value, the limestone aquosity in the area is divided into four grades, i.e., strong, medium, weak, and no aquosity. The regions with resistivity less than 26 Ω•m are determined to be strong aquosity areas, which correspond the green anomalous areas marked 2 and 4 in Figure 7. The region with apparent resistivity from 26 Ω•m to 27 Ω•m is regarded as medium aquosity, which corresponds to the light green anomalous area indicated by 3 in Figure 7. Regions with apparent resistivity in the range of 27 - 60 Ω•m are weak aquosity areas, corresponding to the greenish anomalous areas indicated by 1 and 5 in Figure 7. The regions with apparent resistivity more than 60 Ω•m are not water bearing areas, such as the white area in Figure 7.

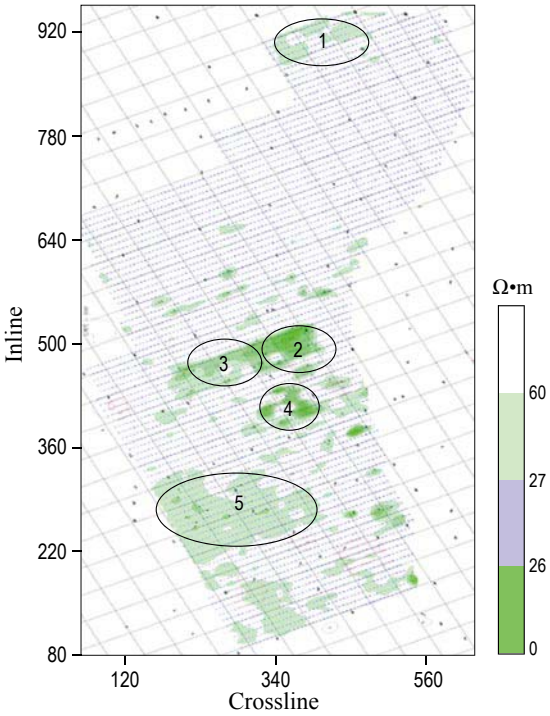

Fig. 7 Transient electromagnetic data 50 m above map limestone top limestone with aquosity areas 1 – 5 from the resistivity data.

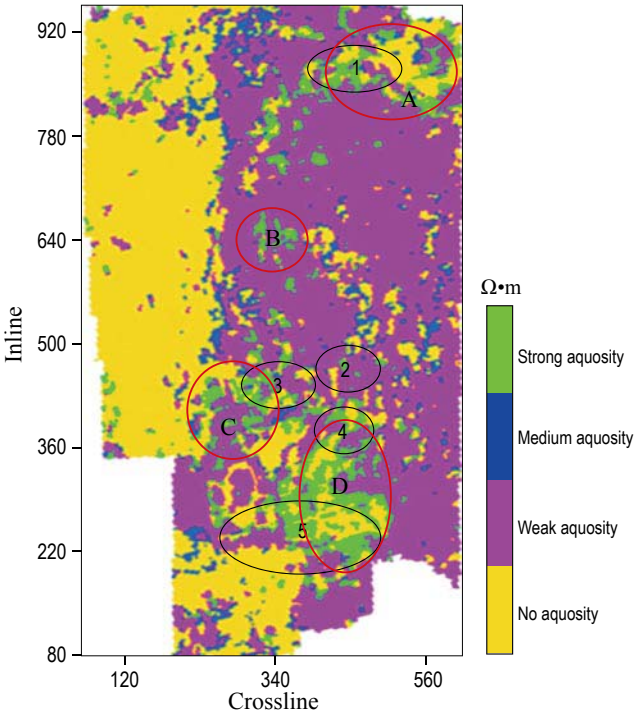

Fig. 8 Predicted limestone aquosity from the neural network.

Comparing the apparent resistivity distribution map (Figure 7) to the attribute maps of Figures 4b, 5b,

and 6b, we find that anomalies 2 and 4 in Figure 7 correspond to the blue area (Figure 4b), to the sky-blue (Figure 5b), and the brown areas. However, from the point of view of the whole exploration area, a single attribute value distribution is not completely consistent with the apparent resistivity map because there are great limitations to using a single attribute for predicting the Ordovician limestone aquosity. For this reason, we predict the Ordovician limestone aquosity using multiple attributes with the constraint of electromagnetic data.

We use the largest Lyapunov exponent, fractal dimension, and entropy attributes as input parameters and perform pattern recognition by BP neural network under the constraint of electromagnetic data. Neural network training and operations are to output four modes, strong, medium, weak, and no aquosity. The output calculated by the neural network is shown in Figure 8. The green region indicates strong aquosity, the blue region indicates medium aquosity, the purple region shows weak aquosity, and the yellow region is no aquosity.

The numbered areas from Figure 7 are superimposed on Figure 8. We find that the abnormal areas from the transient electromagnetic method and the results of multi-attribute prediction are basically consistent. The abnormal area 1 in Figure 7 corresponds with abnormal area A in Figure 8. Abnormal area 3 in Figure 7 corresponds with abnormal area C in Figure 8. Abnormal areas 4 and 5 in Figure 7 correspond with abnormal area D in Figure 8. Anomaly B also was predicted by the multi-attributes. We see that anomaly B also has reflection in the transient electromagnetic map (Figure7) but it is not significant. There is some difference in aquosity range and shape predicted by the two methods but they are basically consistent in general. Thus, our prediction method is correct, the parameters are reasonable, and the results are satisfactory.

Conclusions

From the results of Ordovician limestone aquifer prediction research based on nonlinear seismic attributes, we made the following conclusions:

1. The three seismic attributes: the largest Lyapunov exponent, fractal dimension, and entropy attributes can reflect the complexity of the formation. The research shows that seismic attributes extracted by optimization algorithms can reveal the Ordovician limestone aquosity to a certain extent.

2. With the constraint of other geophysical or log data, the comprehensive analysis of seismic attributes will improve the reliability for prediction of the Ordovician limestone aquosity and reduce the solution uncertainty.

The practical application in the 81st and 82nd coal districts of the Xutuan coal mine demonstrated that the nonlinear seismic attributes can be used for predicting Ordovician limestone aquosity to prevent water inrush during the coalfield production.

Emphasis on research of the inter-relationships between nonlinear seismic attributes and the geological meaning of the target layer and the selection of reasonable seismic attributes by forward modeling methods will be a very important topic in further research.

References

Chopra, S., and Marfurt, K. J., 2005, Seismic attributes: a historical perspective: Geophysics, **70**(5), 3SO – 28SO.

Chopra, S., and Marfurt, K. J., 2006a, Curvature attribute applications to 3D surface seismic data: CSEG Recorder, **31**(7), 44 – 56.

Chopra, S., and Marfurt, K. J., 2006b, Seismic attributes: a promising aid for geological prediction: CSEG Recorder (Special Edition), 115 – 126.

Chopra, S., and Marfurt, K. J., 2007, Volumetric curvature attributes for fault/fracture characterization: First Break, **25**,19 – 30.

Dong, S. H., Ma, Y. L., and Zhou, M., 2004, Forward modeling of relationship between coal seam thickness and seismic attribute of amplitude and frequency: Journal of China University of Mining and Technology, **33**(1), 29 – 32.

Dong, S. H., 2008, Test on elastic anisotropic coefficients of gas coal: Chinese Journal of Geophysics, **51**(3), 254 – 259.

Ge, L. T., and Ye, G. J., 2001, Hydrogeology of China Coal: Coal Industry Press, Beijing, China.

Guo, G. M., 2005, The research and application of the seismic attributes-in the region of Zhaohu nose-like structure of Weibei: PhD Thesis, Southwest Petroleum Institute.

Gui, Z. H., and Han, F. Q., 2004, Wavelet packet-maximum entropy spectrum estimation and its application in turbine's fault diagnosis: Automation of Electric Power Systems, **28**(2), 62 – 66.

Grassberger, P., and Procaccia, I., 1983, Estimation of the Kolmogorov entropy from a chaotic signal: Physical Review Letters, **28**, 2591 – 2593.

Kantz, H., 1994, A robust method to estimate the maximal Lyapunov exponent of a time series: Physics Letters A, **185**(1), 77 – 87.

Lawrence, P., 1998, Seismic attributes in the characterization of small-scale reservoir faults in Abqaiq Field: The Leading Edge, **17**, 521 – 525.

Li, X. R., and Meng, X. D., 2004, Study on fractured karst zone with seismological method: North China Earthquake Sciences, **22**(4), 11 – 12.

Liu, J. L., and Marfurt, K. J., 2007, Instantaneous spectral attributes to detect channels: Geophysics, **72**, 23 – 31.

Liu, X. B., Lin, J. C., and Liu, C. M., 2002, Present conditions and prospects of the researches on seismic reservoir: Acta Geoscientia Sinica, **23**(1), 73 – 78.

Lue, Y. X., 2001, Studying geological significance of seismic attributions use the model technology: Geophysical and Gochemical Exploration, **25**(3), 191 – 197.

Rosenstein, M. T., Collins, J. J., and De Luca, C. J., 1993, A practical method for calculating largest Lyapunov exponents from small data sets: Physica D, **65**(1/2), 117 – 133.

Sukmono, S., 2007, Application of multi-attribute analysis in mapping lithology and porosity in the Pematang-Sihapas groups of Central Sumatra Basin, Indonesia: The Leading Edge, **26**(2), 120 – 131.

Wang, Y. G., Li, Z. C., and Shao, Y., 2000, Reservoirs using seismic data predict fracture zone: Petroleum University (Natural Science Edition), **24**(4), 79 – 82.

Wang, Y. H., and Wen, S., 1996, China coal mine flood prevention and control. Beijing: Coal Industry Press, China, 95 – 110.

Wu, D. K., 1995, Fractal, chaos and catastrophe theory predict oil and gas and applied research: PhD Thesis, Chengdu University of Technology.

Xu, C. B., Qian, J., and Sun, L. X., 2008, Research on seismic interpretation method of karst - fractured zone: Chinese Journal of Engineering Geophysics, **5**(2), 940 – 151.

Yang, D. Q., Jie, M. X., and Wang, Z., 2002, The possibility of detecting water in the Ordovician carbonate with objective seismic exploration: Journal of Coal Society, **27**(1), 36 – 40.

Yi, C. X., 1995, Nonlinear science and its application in the geosciences: Meteorological Press, Beijing, 14 – 32.

Zhang, X. D., 1996, Time series analysis of the higher-order statistics method: Tsinghua University Press, Beijing, 1 – 80.

Huang Yaping received a BS (2005) in Geography Information Systems from China University of Mining And Technology and a MS (2008) in geophysics from China University of Mining and Technology (Xuzhou). Currently he is studying for his PhD at Tongji University of Geophysics. His interests are seismic attribute research and application.